3. A. Fersht, *Enzyme Structure and Mechanism* (Freeman, New York, 1985).
4. U. Englisch *et al.*, *Angew. Chem. Int. Ed. Engl.* **24**, 1015 (1985).
5. S. M. Burgess and C. Guthrie, *Trends Biochem. Sci.* **18**, 381 (1993).
6. A. R. Fersht and C. Dingwall, *Biochemistry* **18**, 2627 (1979).
7. W. Freist, I. Pardowitz, F. Cramer, *ibid.* **24**, 7014 (1985).
8. W. Freist, *ibid.* **28**, 6787 (1989).
9. P. R. Schimmel and D. Söll, *Annu. Rev. Biochem.* **48**, 601 (1979).
10. H. Jakubowski and E. Goldman, *Microbiol. Rev.* **56**, 412 (1992).
11. T. A. Webster, H. Tsai, M. Kula, G. A. Mackie, P. Schimmel, *Science* **226**, 1315 (1984).
12. F. H. Bergmann, P. Berg, M. Dieckmann, *J. Biol. Chem.* **236**, 1735 (1961).
13. A. T. Norris and P. Berg, *Proc. Natl. Acad. Sci. U.S.A.* **52**, 330 (1964).
14. A. N. Baldwin and P. Berg, *J. Biol. Chem.* **241**, 839 (1966).
15. A. A. Schreier and P. R. Schimmel, *Biochemistry* **11**, 1582 (1972).
16. E. W. Eldred and P. R. Schimmel, *J. Biol. Chem.* **247**, 2961 (1972).
17. A. R. Fersht, *Biochemistry* **16**, 1025 (1977).
18. S. Brunie *et al.*, *J. Mol. Graphics* **5**, 18 (1987).
19. P. Brick, T. N. Bhat, D. M. Blow, *J. Mol. Biol.* **208**, 83 (1988).
20. M. A. Rould, J. J. Perona, D. Söll, T. A. Steitz, *Science* **246**, 1135 (1989).
21. S. Brunie, C. Zelwer, J.-L. Risler, *J. Mol. Biol.* **216**, 411 (1990).
22. S. Cusack, C. Berthet-Colominas, M. Härtlein, N. Nassar, R. Leberman, *Nature* **347**, 249 (1990).
23. M. Ruff *et al.*, *Science* **252**, 1682 (1991).
24. R. M. Starzyk, T. A. Webster, P. Schimmel, *ibid.* **237**, 1614 (1987).
25. J. J. Burbaum and P. Schimmel, *Prot. Science* **1**, 574 (1992).
26. K. Shiba and P. Schimmel, *Proc. Natl. Acad. Sci. U.S.A.* **89**, 1880 (1992).
27. E. Schmidt and P. Schimmel, *ibid.* **90**, 6919 (1993).
28. E. Schmidt, unpublished results.
29. Mutations are given by the single-letter code for amino acids. Thus, $Gly^{56} \rightarrow Ala$ is indicated by G56A. Abbreviations for the amino acid residues are: A, Ala; F, Phe; G, Gly; P, Pro; and S, Ser.
30. Mutant or wild-type enzyme was isolated as described (*27, 39*) from cells [strain MI1 (for G56A) or MV1184 (for wild type)] with a multicopy plasmid expressing the desired protein. The reaction mixture contained 100 mM tris-HCl (pH 8.0), 10 mM β-mercaptoethanol, bovine serum albumin (0.1 mg/ml), 0.1 mM EDTA, 10 nM KF, 5 mM $MgCl_2$, 2 mM ATP, 2 mM [^{32}P]sodium pyrophosphate (5.35 to 11.1 cpm/pmol), 0.1 to 40 nM enzyme, and 1 to 1000 μM amino acid (but always under conditions where the amino acid concentration was less than its K_m). Reactions were incubated at 37°C for up to 2 hours. The reaction was quenched with 0.7 volumes of 15% $HClO_4$ and 400 mM sodium pyrophosphate. Activated charcoal was added, and ATP was separated by filtration with 2.4-cm glass fiber pads (Schleicher and Schuell) (*17*).
31. Reactions contained 150 mM tris-HCl (pH 7.5), 10 mM $MgCl_2$, 200 mM valine, 3 mM [γ-^{32}P]ATP (10 to 20 cpm/pmol), pyrophosphatase (2 U/ml), 14 μM $tRNA^{Ile}$, and 2.8 μM enzyme. Reactions were assayed at 25°C for up to 20 min and were quenched with four volumes of 7% $HClO_4$. Activated charcoal containing 10 mM sodium pyrophosphate was added, and ATP was separated by filtration through glass fiber pads (Schleicher and Schuell).
32. *Bacillus stearothermophilus* valine tRNA synthetase was purified from *E. coli* strain MV1184 harboring plasmid pTB8, which encodes the *B. stearothermophilus* enzyme (*40*). The *B. stearothermophilus* enzyme was used to charge *E. coli* $tRNA^{Ile}$ with [^{3}H]valine (*41*). The [^{3}H]valine-$tRNA^{Ile}$ was purified through a series of phenol-chloroform extractions and ethanol precipitations. Deacylation reactions, performed at 25°C, contained 150 mM tris-HCl (pH 7.5), 10 mM $MgCl_2$, 3.25 μM [^{3}H]valine-$tRNA^{Ile}$ (2170 cpm/pmol), pyrophosphatase (4 U/ml), and 5.2 nM enzyme. Aliquots of the reaction mixture were quenched on Whatman 3MM filter pads soaked in 5% trichloroacetic acid (TCA) and then washed repeatedly in 5% TCA and then 100% ethanol to remove free [^{3}H]valine. Under these conditions, the spontaneous rate of valine-$tRNA^{Ile}$ hydrolysis was less than 0.0002 s^{-1}.
33. M. Iaccarino and P. Berg, *J. Bacteriol.* **105**, 527 (1971).
34. G. Treiber and M. Iaccarino, *ibid.* **107**, 828 (1971).
35. The F570S mutation was identified through the sequencing of the PCR-amplified *ileS* gene of the MI1 strain (*42*). For protein purification, the mutation was introduced into the IleRS coding sequence of pKS21 and the mutant protein was expressed from the plasmid in *E. coli* strain IQ844 (*26*).
36. G. Ghosh, H. Pelka, L. Schulman, S. Brunie, *Biochemistry* **30**, 9569 (1991).
37. Y.-M. Hou, K. Shiba, C. Mottes, P. Schimmel, *Proc. Natl. Acad. Sci. U.S.A.* **88**, 976 (1991).
38. J. J Burbaum and P. Schimmel, *J. Biol. Chem.* **266**, 16965 (1991).
39. A. Shepard, K. Shiba, P. Schimmel, *Proc. Natl. Acad. Sci. U.S.A.* **89**, 9964 (1992).
40. T. J. Borgford, N. J. Brand, T. E. Gray, A. R. Fersht, *Biochemistry* **26**, 2480 (1987).
41. R. Giegé *et al.*, *Eur. J. Biochem.* **45**, 351 (1974).
42. V. Murray, *Nucleic Acids Res.* **17**, 8889 (1989).

43. We thank A. Fersht, W. Freist, R. Giegé, and H. Jakubowski for reading and commenting on this manuscript before its submission for publication. Plasmid pTB8 was a gift of T. Borgford. This work was supported by NIH grant GM 15539. E.S. is an NIH predoctoral trainee.

3 December 1993; accepted 2 March 1994

Stimulation of Human γδ T Cells by Nonpeptidic Mycobacterial Ligands

Patricia Constant, François Davodeau, Marie-Alix Peyrat, Yannick Poquet, Germain Puzo, Marc Bonneville, Jean-Jacques Fournié*

Most human peripheral blood γδ T lymphocytes respond to hitherto unidentified mycobacterial antigens. Four ligands from *Mycobacterium tuberculosis* strain H37Rv that stimulated proliferation of a major human γδ T cell subset were isolated and partially characterized. One of these ligands, TUBag4, is a 5′ triphosphorylated thymidine-containing compound, to which the three other stimulatory molecules are structurally related. These findings support the hypothesis that some γδ T cells recognize nonpeptidic ligands.

Since the discovery of the γδ T cell receptor (TCR), various studies have demonstrated the involvement of γδ T lymphocytes in immune responses to mycobacteria (*1*). The nature of antigens recognized by γδ T cells has remained elusive, as has the physiological function of these cells. In mice, γδ T cells derived from lung and newborn thymus respond to tuberculin and to hsp65-derived peptides, suggesting a specialized role in stress immunity (*2*). In humans, though some γδ T lymphocytes reactive to mycobacteria recognize hsp65 (*3*), most of them appear to have different unidentified ligands (*4*). Such ligands recovered in hydrosoluble extracts from *Mycobacterium tuberculosis* have small molecular masses (1 to 3 kD) and, on the basis of several lines of indirect evidence, were assumed to be carbohydrate in nature (*5*). Here, we show that these ligands are phosphorylated molecules related to a thymidine 5′-triphosphoryl-X nucleotide conjugate.

Isolation of the stimulating ligands in hydrosoluble extracts from *M. tuberculosis* strain H37Rv cultures [mycobacterial extracts (ME)] was monitored by the proliferative response of a mycobacteria-reactive human γδ T cell clone, G115 (*6*). To determine the chemical nature of the ligands, we submitted ME to various treatments. The ligands were resistant to proteases as described (*5*) but sensitive to periodic acid oxidation and to alkaline phosphatase (*7*). Fractions from gel permeation chromatography of ME were analyzed for carbohydrate content and biological activity (Fig. 1A). The stimulating fractions appeared in two broad overlapping peaks containing carbohydrate, with an estimated mass range of 500 to 600 daltons. Taken together, these preliminary findings suggested that the stimulating ligands for the γδ T cell clone G115 were small phosphorylated glycoconjugate molecules.

These ligands were purified from ME by anion exchange chromatography, silicic acid chromatography, and C18 ion-pair reversed-phase high-pressure liquid chromatography (rpHPLC). With this procedure, four biologically active components, named TUBag1 to TUBag4 according to

P. Constant, Y. Poquet, G. Puzo, J.-J. Fournié, Department III, Laboratoire de Pharmacologie et de Toxicologie Fondamentales du CNRS, 118, Rte de Narbonne, 31062 Toulouse, France.
F. Davodeau, M.-A. Peyrat, M. Bonneville, INSERM U211, Institut de Biologie, 9, Quai Moncousu, 44035 Nantes, France.

*To whom correspondence should be addressed.

their increasing hydrophobicity, were separated into discrete peaks (Fig. 1B). Because parallel diode array detection at variable wavelength revealed contaminating compounds in most fractions, repeated chromatography of each activating TUBag was needed to purify the components to homogeneity. With this protocol, we obtained about 50 μg of the biologically active component TUBag4 from 12 liters of *M. tuberculosis* H37Rv cultures. As for the other three components, TUBag2 and TUBag3 were not obtained in sufficient amounts to allow structural analysis and TUBag1, which eluted close to the HPLC solvent peak, could not be purified to homogeneity. High pH anion exchange chromatographic (HPAEC) analysis of TUBag4 revealed a single peak, detected by chemical-suppressed ion conductivity (Fig. 1C), which by itself was capable of stimulating clone G115 (*8*). We considered this TUBag4 sample, which yielded a single peak in both C18 rpHPLC and HPAEC, to be purified to homogeneity.

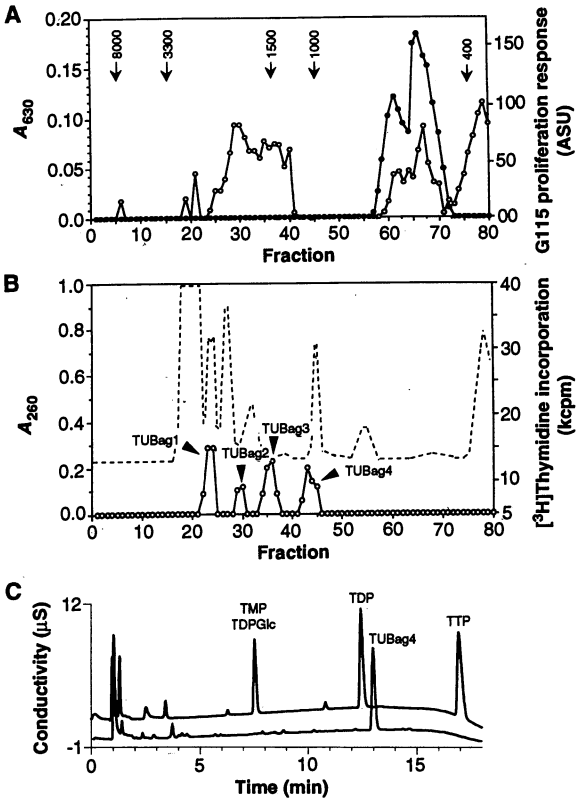

Fig. 1. (**A**) Size permeation chromatography of *M. tuberculosis* antigens. Samples (100 mg) of ME were loaded on an Ultrogel AcA202 (1/130 cm) column eluted with 0.1 M ammonium acetate. Fractions (1 ml) were collected, assayed for carbohydrates with sulfuric anthron and absorbance at 630 nm (A_{630}) (○), and assayed for G115 clone stimulation (●). Upper arrows indicate molecular weights of polyethylene standards. Arbitrary stimulation units (ASU) were defined as the highest sample dilution inducing half-maximal proliferation of clone G115. (**B**) Separation of four antigens from ME. The biologically active fraction (100 mg) from the ME separation on DEAE was chromatographed with ion-pair preparative C18 rpHPLC (10 μm, 20/250 mm column) and ammonium acetate (0.1 M) eluent. We monitored absorption at variable wavelength with a diode array detector ($A_{260\ nm}$, shown by dotted line) and monitored stimulating activity on the G115 clone as incorporation of [^{3}H]thymidine, thousands of counts per minute (kcpm) (○). Stimulating fractions from the same antigen were pooled and termed as indicated. (**C**) Analysis by HPAEC of TUBag4 purified by C18 rpHPLC. About 1 μg of TUBag4 was chromatographed (lower profile) on a Dionex DX300 apparatus with an Ion Pac AS11 (4 mm) anion exchange column, with NaOH (0.1 M) and CH_3CN gradients in water detected by conductivity in the chemical suppression mode. Standards (upper profile) of thymidine 5′-monophosphate or thymidine 5′-diphosphate glucose (respectively, TMP and TDPGlc, 7.5 min), thymidine 5′-diphosphate (TDP, 12.4 min), and thymidine 5′-triphosphate (TTP, 16.9 min) chromatographed differently from TUBag4 (13.0 min).

Table 1. The effect of mAbs to TCR on TUBag4-triggered amplification of $V_\gamma9$ $V_\delta2$ PBLs. Freshly isolated PBLs from a healthy donor were cultured for 10 days in interleukin-2–supplemented medium in the absence or presence of TUBag4 and mAb (1/100 ascites): IH1, antibody to $V_\delta1$ (*21*); 510, pan δ (*19*); 360, anti-$V_\gamma9$ (*19*); and 389, anti-$V_\delta2$ (*19*). Live cells in the cultures were then counted and phenotyped by indirect immunofluorescence with various TCR-specific mAbs and flow cytometry. Results are expressed as percent of positive cells for a given mAb. Absolute numbers of γδ T cells in each culture demonstrate blocking of the TUBag4-triggered amplification. None of these mAbs to TCR affected the phytohemagglutinin lectin–induced proliferative activity of the $V_\gamma9$ $V_\delta2$ T cell clone G115 (*21*), suggesting that the mAb-mediated blocking of cell amplification was specific for the TUBag4 stimulus. The increased background staining of PBLs cultured with mAbs 510, 360, and 389 is due to persistence of these mAbs added to cultures, as indicated by staining with only fluorochrome-conjugated antibody to mouse immunoglobulin.

Culture conditions	Percent of cells expressing the following V or C chain					Absolute number of Cδ$^+$ cells ($\times 10^{-4}$)
	None	$V_\delta1$	C_δ	$V_\gamma9$	$V_\delta2$	
Medium	0.2	0.4	5.5	3.8	3.9	3.6
TUBag4	0.7	0.5	28.3	25.8	25.4	41.0
+ IH1	0.8	0.6	20.3	19.1	19.9	34.7
+ 510	3.9	4.2	4.3	4.6	4.4	7.1
+ 360	2.8	2.8	4.6	3.4	2.4	6.9
+ 389	3.7	4.4	5.4	3.7	4.4	9.5

Structural analysis of TUBag4 was undertaken with one-dimensional and two-dimensional homo- and heteronuclear magnetic resonance (NMR). One-dimensional ^{1}H spectrum of TUBag4 (Fig. 2A) revealed the reporter groups of 2-deoxyribose, such as H-1 (*t*, δ 6.280 ppm, $J_{1,2,2'}$ 6.4 Hz) and H-2,2′ (*m*, δ 2.309 ppm), and of thymine, such as H-6 (*s*, δ 7.677 ppm). Using two-dimensional homonuclear ^{1}H correlated spectroscopy (COSY) and homonuclear Hartman-Hahn (HOHAHA) spectroscopy and ^{1}H-^{13}C heteronuclear multiple-quantum coherence (HMQC) and heteronuclear multiple-bond correlation (HMBC) experiments with gradient pulse techniques, we were able to assign the ^{1}H and ^{13}C chemical shifts (*9*). From these data we identified the structure of thymidine in TUBag4, and the chemical shifts suggested the presence of 5′ phosphate and excluded 3′ phosphate substitution (*10*). Direct insertion probe electron impact–mass spectrometry (EI-MS) was used to confirm the presence of phosphate in TUBag4 (*11*). The EI-MS spectrum of the per-trimethylsilyl (TMS) derivative of TUBag4 showed intense peaks at *m/z* 211 and *m/z* 299, characteristic of phosphate groups (Fig. 2B), and the peaks at *m/z* 126 and *m/z* 155 confirmed the presence of thymidine. Taken together, these results suggested that TUBag4 contains thymidine 5′-phosphate; however, when biologically tested with the clone G115, thymidine, thymidine monophosphate (TMP), thymidine diphosphate (TDP), and thymidine triphosphate (TTP) standards were inactive, revealing that TUBag4 was not composed solely of phosphorylated thymidine. Moreover, these data could not reveal whether 5′-di- or 5′-triphosphate was present in this molecule. We resolved this issue by using both chromatography and enzymatic degradation (*12*). Native TUBag4 eluted on C18 ion-pair rpHPLC between TDP and TDPGlc and was unaffected by alkaline phosphatase treatment (Fig. 2C). Given that TUBag4, which has an estimated mass of 500 to 600 daltons (Fig. 1A), does not contain any terminal phosphate monoester, this left only the two possible structures TDP-X or TTP-X. Two indirect pieces of evidence

suggested that TUBag4 has the TTP-X structure: (i) from comparative HPAEC analysis, TUBag4 elutes (13.0 min) after TDP (12.4 min), whereas TDPGlc coelutes with TMP (Fig. 1C), and (ii) free phosphate was detected with HPAEC analysis of the venom nucleotide pyrophosphatase products of either TDP, TTP, or TUBag4 but not of TDPGlc.

On treatment with venom nucleotide pyrophosphatase (*12*), TUBag4 was degraded into TMP and a biologically active component that behaved like TUBag1 in both C18 rpHPLC (Fig. 2C) and HPAEC (*13*). In contrast to TUBag4, alkaline phosphatase treatment completely abolished TUBag1 biological activity (*7*), ruling out any exclusive contribution of the X moiety to TUBag4 activity. TUBag2 and TUBag3 are related phosphorylated metabolites: TUBag2, like TUBag1, was inactivated by alkaline phosphatase, and TUBag3 appears to be of a nucleotide conjugate nature because it was inactivated by venom nucleotide pyrophosphatase (*14*). Therefore, the partial alkaline phosphatase sensitivity of crude TUBag mixture can be interpreted as loss of TUBag1 and TUBag2 activities, whereas the complete abrogation of TUBag activity after periodic acid treatment can be explained by the sensitivity of phosphate and pyrophosphate diesters to acids. Structure of the X residue remains to be determined, but this is hampered by the very low amounts of highly purified molecules that can be recovered from large volumes of *M. tuberculosis* cultures.

When titrating the biological activity of purified TUBag4, the minimal TUBag4 concentration required for half-maximal proliferative response of clone G115 was ~1 ng/ml [that is, 2 nM for an estimated mass of 500 daltons (Fig. 3A)]. To assess the biological activity of purified TUBag4, we assayed for the selective amplification of γδ T cells after short-term bulk cultures of peripheral blood lymphocytes (PBLs) from four healthy donors. TUBag4 induced a 40- to 500-fold amplification of γδ T cell numbers after a 10-day culture, but had no effect on αβ T lymphocytes and $CD3^-$ cell proliferation (Fig. 3B). In agreement with earlier reports (*15*), the T cell population amplified with TUBag4 expressed a TCR comprising $V_\gamma 9$ and $V_\delta 2$ variable (V) regions (Fig. 3C). Moreover, TUBag4-mediated amplification of $V_\gamma 9$ $V_\delta 2$ T lymphocytes was specifically blocked by monoclonal antibodies (mAbs) directed against either $V_\gamma 9$, $V_\delta 2$, or C_δ TCR chains (anti-$V_\gamma 9$, -$V_\delta 2$, -C_δ, respectively) (Table 1). These results suggest that TUBag4 stimulates in a TCR-dependent fashion a powerful polyclonal response of a major peripheral γδ T cell subset in humans.

The nature of the mycobacterial ligands for γδ T lymphocytes remained an unre-

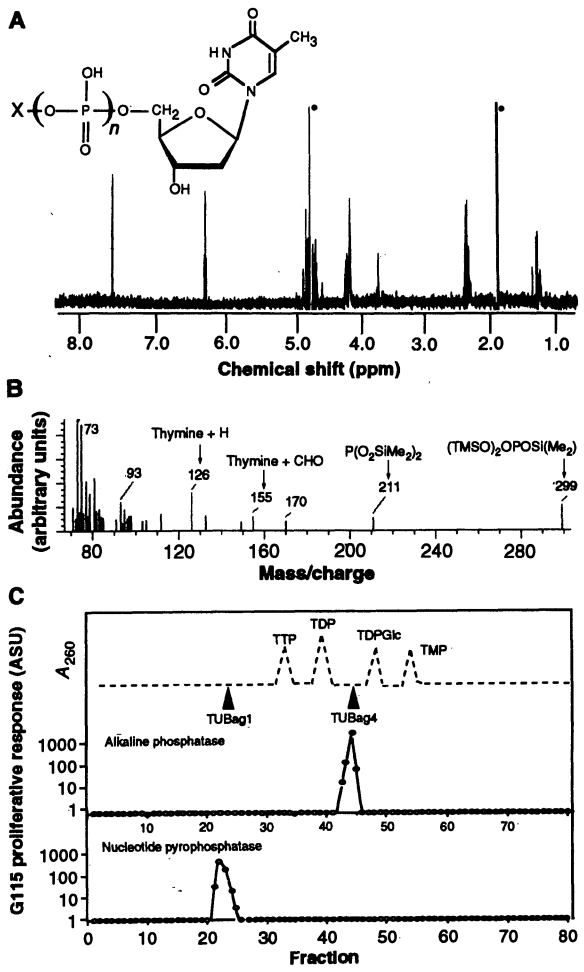

Fig. 2. (**A**) The ^1H NMR spectrum of TUBag4. (A 50-μg sample in D_2O, Bruker AMX 500 MHz.) Spotted peaks are from HOD and ammonium acetate. Complete assignments of the chemical shifts were obtained from COSY, HOHAHA, HMBC, and HMQC experiments (*9*): for thymine: H-6, 7.677 ppm; methyl-5 (Me-5), 1.9 ppm (with ammonium acetate peak); C-2, 150.4 ppm; C-4, 165.3 ppm; C-5, 110.0 ppm; C_{Me-5}, 10.4 ppm; and C-6, 136.2 ppm. For 2-deoxyribose: H-1, 6.280 ppm; H-2,2′; 2.309 ppm; H-3, 4.558 ppm; H-4, 4.096 ppm; H-5,5′, 4.096 ppm; C-1, 83.81 ppm; C-2, 37.58 ppm; C-3, 69.6 ppm; C-4, 84.4 ppm; and C-5, 64.15 ppm. These findings are in agreement with published data about thymidine 5′-phosphate (*10*). (**B**) AnEI-MSspectrumofper-trimethylsilylated TUBag4. (A 1-μg sample Hewlett-Packard 5989A, 70 eV, direct insertion probe temperature of 290°C.) Evidence for the presence of phosphate in TUBag4 was provided from *m/z* 299 or *m/z* 211 rearrangement ions indicated above, and the presence of peaks at *m/z* 126 and *m/z* 155 confirm the occurrence of thymidine (*11*). (**C**) Enzymatic degradation of TUBag4. Biological activity of C18 rpHPLC fractions (same HPLC conditions as in Fig. 1B) from TUBag4 treated with the above-specified enzymes (*12*). The upper dotted line shows a C18 rpHPLC profile of TTP, TDP, TDPGlc, and TMP, and arrows indicate the eluting positions for TUBag1 and TUBag4.

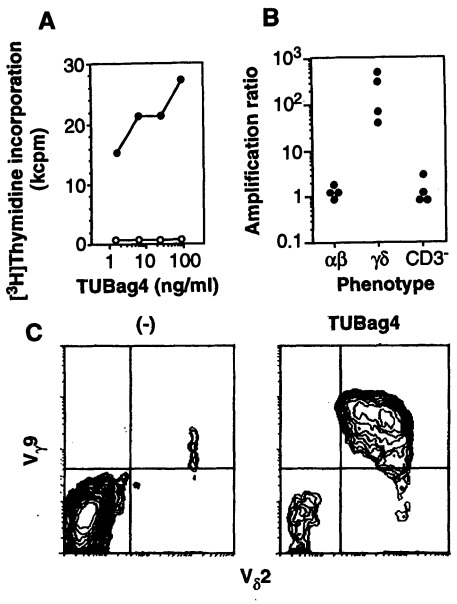

Fig. 3. (**A**) Proliferative response of clone G115 to TUBag4. The G115 cells (10^4 per well) were cultured for 72 hours in the presence of irradiated B-LCL cells (2.5 × 10^4 per well) and recombinant interleukin-2 (rIL-2, 75 U BRMP) in RPMI plus 10% pooled human serum. TUBag4 (●) or negative control sample (○, TDP) was added to the cultures at the concentration specified. Specific [^{3}H]thymidine incorporation was obtained for each sample by subtracting counts per minute of cultures without antigen. (**B**) Selective in vitro amplification of γδ PBLs by TUBag4. PBLs from four healthy donors were cultured in rIL-2–supplemented medium in the absence or presence of TUBag4 (saturating amounts). After being cultured for 10 days, cells were counted and phenotyped by indirect immunofluorescence with the pan-β mAb BMA 031 and the pan-δ mAb 510 (*19*). The amplification ratio (*R*) was calculated according to the following formula: $R = (N_{TUB} \times A_{TUB})/(N_{med} \times A_{med})$, where N_{TUB} and N_{med} correspond to the total number of cells recovered after culture with or without TUBag4, respectively, and *A* corresponds to the percent of cells recognized by a given mAb (*20*). (**C**) The γδ T cell population amplified after culture with TUBag4 expressed TCR $V_\gamma 9$ and $V_\delta 2$ regions. The PBLs from donor 2 (*20*) were phenotyped by two-color immunofluorescence with the $V_\gamma 9$-specific mAb 360 (*19*) and the $V_\delta 2$-specific mAb 389 (*19*) and analyzed by flow cytometry with a Becton Dickinson FACScan and Lysys II software. Shown are the contour plots of red ($V_\gamma 9$) fluorescence versus green ($V_\delta 2$) fluorescence on a log-log scale obtained from cells cultured in the absence (left) or presence of TUBag4 (right).

solved and controversial question. Selective stimulation of γδ T cells by carbohydrates has been suggested (*16*). Our studies demonstrate that these ligands are phosphorylated metabolites of a thymidine-containing nucleotide conjugate named TUBag4. To our knowledge, thymidine-containing nucleotide conjugates had not been previously reported in nature. They may be involved in a metabolic pathway related to DNA, such as cell proliferation or nucleic acid repair. Such molecules would fit with the "stress antigens" or "conserved primitive stimuli" theoretically expected for γδ T lymphocytes (*17*). Understanding their metabolic function in the producing cell may help to elucidate the physiological role of reactive γδ T cells. Our results may also provide clues to understanding autoimmune diseases, for example, T cell help for production of pathogenic immunoglobulin G to DNA in lupus patients frequently involves γδ T cells (*18*), and this may be triggered by TUBags or structurally related stimuli.

REFERENCES AND NOTES

1. E. M. Janis, S. H. E. Kaufmann, R. H. Schwartz, D. M. Pardoll, *Science* **244**, 713 (1989); R. L. Modlin *et al.*, *Nature* **339**, 544 (1989).
2. R. A. O'Brien *et al.*, *Cell* **57**, 667 (1989); A. Augustin, R. T. Kubo, G. K. Sim, *Nature* **340**, 239 (1989); M. P. Happ, R. T. Kubo, E. Palmer, W. K. Born, R. L. O'Brien, *ibid.* **342**, 696 (1989); W. Born *et al.*, *Science* **249**, 67 (1990); W. Born *et al.*, *Immunol. Today* **11**, 40 (1990).
3. A. Haregewoin, G. Soman, R. C. Hom, R. W. Finberg, *Nature* **340**, 309 (1989); P. Fisch *et al.*, *Science* **250**, 1269 (1990); P. Fisch *et al.*, *J. Immunol.* **148**, 2315 (1992); I. Kaur *et al.*, *ibid.* **150**, 2046 (1993).
4. H. Holoshitz, F. Konig, J. E. Coligan, J. De Bruyn, S. Strober, *Nature* **339**, 226 (1989); D. Kabelitz, A. Bender, S. Schondelmaier, B. Schoel, S. H. E. Kaufmann, *J. Exp. Med.* **171**, 667 (1990).
5. K. Pfeffer, B. Schoel, H. Gulle, S. H. E. Kaufmann, H. Wagner, *Eur. J. Immunol.* **20**, 1175 (1990); K. Pfeffer *et al.*, *J. Immunol.* **148**, 575 (1992).
6. F. Davodeau *et al.*, *J. Immunol.* **151**, 1214 (1993).
7. P. Constant *et al.*, data not shown.
8. The peak detected at 13.0 min in HPAEC analysis of TUBag4 was collected, and its ability to stimulate clone G115 (measured in arbitrary stimulation units) matched that of total TUBag4 before HPAEC separation.
9. Each individual ^{13}C chemical shift was obtained through its coupling with correlated ^{1}H signals during the heteronuclear HMQC and HMBC experiments. The linkage of 2-deoxyribose with thymine was established from HMBC results, as the ^{1}H δ 6.280-ppm signal (2-deoxyribose H-1) correlates with a ^{13}C signal at δ 136 ppm (thymine C-6), whereas the ^{1}H δ 7.677-ppm signal (thymine H-6) correlates with the following ^{13}C signals: δ 10.46 ppm (thymine Me-5), δ 83.81 ppm (2-deoxyribose C-1), δ 150.4 ppm (thymine C-2), and δ 165.3 ppm (thymine C-4); P. Constant, M. Gilleron, J. Vercauteren, J.-J. Fournié, unpublished data.
10. E. Breitmaier and W. Voelter, *Carbon-13 NMR Spectroscopy*, (VCH, Weinheim, Federal Republic of Germany, VCH, ed. 3, 1987), pp. 401–414.
11. J. A. McCloskey, in *Basic Principles in Nucleic Acid Chemistry*, P. O. P. Tso', Ed. (Academic Press, New York, 1974), vol. I, chap. 3.
12. Phosphatase reactions were done with either 3 U of calf intestine alkaline phosphatase (Boehringer type 713023) or nucleotide pyrophosphatase from *Crotalus adamanteus* venom (Sigma type II, 0.5 U) incubated in 100 μl of 50 mM tris (pH 8.4) at 37°C for 120 min.
13. Similar HPAEC retention times were found when comparing the biologically active fractions of TUBag1 chromatography with those from venom nucleotide pyrophosphatase-treated TUBag4.
14. P. Constant, Y. Poquet, M. A. Peyrat, M. Bonneville, J.-J. Fournié, unpublished data.
15. D. Kabelitz *et al.*, *J. Exp. Med.* **173**, 1331 (1991).
16. D. H. Raulet, *Nature* **339**, 342 (1989); J. L. Strominger, *Cell* **57**, 895 (1989); W. Haas, P. Pereira, S. Tonegawa, *Annu. Rev. Immunol.* **11**, 637 (1993).
17. C. A. Janeway Jr., B. Jones, A. Hayday, *Immunol. Today* **9**, 73 (1988).
18. S. Rajagopalan, T. Zordan, G. C. Tsokos, S. K. Datta, *Proc. Natl. Acad. Sci. U.S.A.* **87**, 7020 (1990).
19. F. Davodeau *et al.*, *J. Biol. Chem.* **268**, 15455 (1993).
20. The proportion of γδ cells after culture without TUBag4 versus with TUBag4 were the following: donor 1, 0.9/69.5; donor 2, 2.6/86.5; donor 3, 5.0/74.1; and donor 4, 1.0/27.2. After culture with TUBag4, γδ cells from all donors tested expressed $V_\gamma 9$ and $V_\delta 2$ regions (Fig. 3 C) (*21*).
21. F. Davodeau, M. A. Peyrat, M. Bonneville, unpublished data.

22. We thank M. A. Laneelle for cultures of *M. tuberculosis* H37Rv; M. Gilleron and J. Vercauteren for NMR experiments; and G. Tuffal R. Albigot, A. Godart, Y. Jacques, M. Daffé, and P. Lerouge for technical advice. This work is part of the doctorat de l'Université Paul Sabatier (P.C.). Supported in part by the World Health Organization and United Nations Development Programme for Vaccine Development (IMMTUB n°92TB0028), l'Association pour la Recherche contre le Cancer (ARC 6690), and institutional grants from the CNRS (Interface Chimie-Biologie) and la Région Midi-Pyrénées (RECH/ 9200841).

2 November 1993; accepted 1 February 1994

Telomere-Led Premeiotic Chromosome Movement in Fission Yeast

Yuji Chikashige, Da-Qiao Ding, Hironori Funabiki, Tokuko Haraguchi, Shinro Mashiko, Mitsuhiro Yanagida, Yasushi Hiraoka

The movement of chromosomes that precedes meiosis was observed in living cells of fission yeast by fluorescence microscopy. Further analysis by in situ hybridization revealed that the telomeres remain clustered at the leading end of premeiotic chromosome movement, unlike mitotic chromosome movement in which the centromere leads. Once meiotic chromosome segregation starts, however, centromeres resume the leading position in chromosome movement, as they do in mitosis. Although the movement of the telomere first has not been observed before, the clustering of telomeres is reminiscent of the bouquet structure of meiotic-prophase chromosomes observed in higher eukaryotes, which suggests that telomeres perform specific functions required for premeiotic chromosomal events generally in eukaryotes.

The centromere is generally believed to be a unique chromosomal site that leads the chromosome movement. Here we report a situation in which telomeres proceed first in the direction of travel during chromosome movement. We examined the chromosome dynamics during the process of meiosis in living and fixed cells of fission yeast by the use of a computerized fluorescence microscope system with a cooled charge-coupled device (CCD). Our results reveal that telomeres cluster at the leading end of the chromosome movement during premeiotic stages.

In fission yeast *Schizosaccharomyces pombe*, haploid cells of the opposite mating type, h^+ and h^-, conjugate upon nitrogen starvation and enter the process of meiosis (zygotic meiosis); alternatively, h^+/h^- diploid cells can be directly induced to undergo meiosis (azygotic meiosis) (*1–3*). A characteristic elongated nuclear morphology, generally called horse tail, is observed during a certain period preceding meiotic divisions (Fig. 1) (*4*). The horse-tail period includes meiotic prophase defined in higher eukaryotes, during which the association and recombination of homologous chromosomes take place (*1, 2*).

We first examined chromosome dynamics during meiosis in individual living cells. Fission yeast cells were induced to undergo meiosis and stained with a DNA-specific fluorescent dye, Hoechst 33342; meiotic processes in the stained cells were allowed to proceed on a microscope slide (*5*). In live meiosis, the noticeable movement of nuclei was observed during karyogamy and the horse-tail period. Selected frames of chromosome dynamics in zygotic meiosis are shown for the period of karyogamy (Fig. 2A) and for the horse-tail (Fig. 2B) and meiotic chromosome segregations (Fig.

Y. Chikashige, D.-Q. Ding, T. Haraguchi, S. Mashiko, Y. Hiraoka, Kansai Advanced Research Center, Communications Research Laboratory, 588-2 Iwaoka, Iwaoka-cho, Nishi-ku, Kobe 651-24, Japan.
H. Funabiki and M. Yanagida, Department of Biophysics, Faculty of Science, Kyoto University, Kyoto 606, Japan.